Primljen / Received: 10.10.2023.
Ispravljen / Corrected: 25.3.2024.
Prihvaćen / Accepted: 3.4.2024.
Dostupno online / Available online: 10.6.2024.

Effect of pillar size and joint dip on stability of porous limestone cellars

Authors:

Jalal Zenah, PhD Candidate
Budapest University of Technology and Economics
Faculty of Civil Engineering
Department of Engineering Geology and Geotechnics
jalal.zenah@edu.bme.hu
Corresponding author

Assoc.Prof. **Péter Görög**, PhD. CE
Budapest University of Technology and Economics
Faculty of Civil Engineering
Department of Engineering Geology and Geotechnics
gorog.peter@emk.bme.hu

Professional paper

Jalal Zenah, Péter Görög

Effect of pillar size and joint dip on stability of porous limestone cellars

Pillars play an essential role in the stability of an underground cavity. Their most important parameters are the dimensions, material parameters, condition, and joint geometry. This research investigates the impact of geometrical horizontal cross section and joint's dip angle on the stability of the pillar, which affects the stability of cavities. The chosen study site is in a cellar system in Budapest, Hungary. According to the laboratory and on-site investigations, the cellar's host rock is porous limestone with a low strength but a massive rock mass with few discontinuities. In some of the previously investigated cellar systems the edge of the pillars was cut because of space requirements. Therefore, this study aims to determine the effect of such geometrical changes on the stability of the cellar. A 25 m2 room with a single square-based pillar was used to model the stability. Material parameters were determined through various laboratory tests such as UCS, triaxial, and discontinuity shear strength tests, as well as rock mass classification. Three-dimensional finite element software (RS3) was used to evaluate the stability of the studied pillar. Overall, this study provides valuable insights into the factors that influence stability of pillars in underground cavities and highlights the importance of carefully considering these factors when designing, verifying, and constructing support systems for underground structures.

Key words:
3D, pillar, stability, joints, numerical modelling, RS3, dip angle, width and height ratio

Stručni rad

Jalal Zenah, Péter Görög

Učinak veličine stupa i kuta nagiba pukotina na stabilnost podzemnih prostorija u poroznim vapnencima

Stupovi imaju ključnu ulogu u stabilnosti podzemnih prostorija. Njihovi najvažniji parametri uključuju dimenzije, parametre materijala, stanje i geometriju pukotina. U ovom se radu ispituje utjecaj geometrijskog horizontalnog presjeka i kuta nagiba pukotina na stabilnost stupa, što utječe na stabilnost prostorija. Odabrano mjesto ispitivanja nalazi se u podrumskim sustavima u Budimpešti u Mađarskoj. Prema laboratorijskim istraživanjima i istraživanjima na terenu, matična stijena prostorija je porozni vapnenac male čvrstoće, ali predstavlja masivnu stijensku masu s malo diskontinuiteta. U nekima od prethodno istraženih podrumskih sustava, rub stupova je odrezan zbog prostornih potreba. Stoga je cilj ovog rada utvrditi učinak takvih geometrijskih promjena na stabilnost prostorija. Za modeliranje stabilnosti upotrijebljena je prostorija veličine 25 m^2 s jednim kvadratnim stupom. Parametri materijala određeni su različitim laboratorijskim ispitivanjima kao što su UCS, troosna ispitivanja, ispitivanja posmične čvrstoće diskontinuiteta te klasifikacijom stijenske mase. Ovaj rad pruža dragocjen uvid u čimbenike koji utječu na stabilnost stupova u podzemnim prostorijama te naglašava važnost pažljivog razmatranja tih čimbenika pri projektiranju, provjeri i izgradnji potpornih sustava za podzemne građevine.

Ključne riječi:
3D, stup, stabilnost, pukotine, numeričko modeliranje, RS3, kut nagiba, odnos širine i visine

1. Introduction

The stability of underground cavities is of utmost importance, as unstable cavities can lead to collapses, sinkholes, and other dangerous conditions. Pillars play a critical role in supporting the weight of the overburden, which is the rock and soil that covers the cavity. Without a stable pillar system, the ground and the building above it are in danger [1]. It is impossible to control the ground and overburden without stable pillars [2].

Pillars can be defined as in-situ rock mass between two or more underground openings, which are created due to the construction of an underground mine in variable geometries [3]. The pillar's geometry affects underground cavities' safety [4]. The ratio width-to-height (W/H) has been defined as an influenced parameter on pillar strength and its potential failure mode [5].

The research aims to determine the critical width of the column pillar in the presence of joints in different dip angles to achieve the stability requirement of the cellar. The pillars' width changed because of the need for more space inside the cellar, which could cause cellar instability and subsidence at the ground surface above it. The model is created based on a real cellar under a new construction area by changing the width of a pillar to achieve the relation between the cellar's stability and the pillar's width. The stability analysis of this work was done by the Rocscience software package with the RS3 FEM program.

The studied cellar system is hosted by porous limestone, which, according to its name, is highly porous and easy to work with [6], There is some previous research which investigated the physical and mechanical properties of this rock and compared the different laboratory test results [6-8]. Using rock mass classification tools is important to determine the strength and stiffness parameters for the jointed, weathered, sometimes crushed porous limestone layers above the cellar roof. The Geological Strength Index was applied for this by using previous experiences. The usage of GSI for different kinds of rock masses is introduced as in referenced research [9], and the comparison of different calculation methods of GSI was done as in refernecd research [10].

The stability of the various types of pillars in different materials has been studied previously like coal pillars [2, 11, 12], sandstone pillars USA [13, 14], a pillar in hematite mine [15], a coal mine in western Pennsylvania USA [16], coal mining in Greece [17], a pillar in a limestone mine in South Korea [18], a pillar in a gold mine in Colombia [19], a crown pillar in Canada [20], South Africa [21], and in India [22], slender column pillar in limestone [23]. Numerical modelling helps to evaluate the cavities; after field investigations the evaluations of numerical modelling are considered to be a useful tool for rock mass characterisation [24].

Jessu and Spearing [25] used three-dimensional finite difference numerical modelling (FLAC3D) to simulate the vertical and inclined column pillars and analyse the pillar strength reduction in the presence of discontinuities. Four different width-to-height (W/H) ratios (0.5, 1.0, 1.5 and 2.0) were studied by changing the dip angle of discontinuity.

Le Quang et al. [26] studied the displacements of the cellars under the load of a road, which developed because of the change in pillar width.

The cellars in the studied area have both column and wall pillars. The problem arises when the horizontal cross-section of the pillars is reduced to create more space inside the cellar, as shown inFig. 1. This reduction in cross-section can lead to stability problems in both the cellar and the area above it, which is planned to be built; therefore, an extra load is expected on the pillars. Any reduction in their cross-section can compromise the ability of the pillar to support the load above, which can cause stability problems. This can lead to structural failure which can be dangerous and potentially life-threatening.

Figure 1. The cut pillars in the studied area

Different sizes of pillars and various orientations of joints are considered in the calculations to investigate the effect of the geometrical changes shown in Figure 1 and the joint orientation on the stability of the pillar. During mining activities, when the mine or part of the mine is abandoned, the dimensions of the pillars are reduced to extract some of the material from the pillar. This process can cause the same effect on stability, but long-term stability is not required in mining projects.

2. Geological description

The studied cellars were located in Budafok, south of Budapest, Hungary, where a lot of cellars were cut under this area in Miocene porous limestone.

The studied Hungarian limestone is porous [27] and formed during the Miocene period. The limestone is considered a shallow marine subtropical carbonate deposited in the Pannonian Basin. It covers larger areas in and around Budapest [8]. It was used as a construction material for centuries, and emblematic buildings of Budapest, such as the Parliament building, Citadella Fortress and Mathias Church, were built from this stone [27].

The tested porous Miocene limestone is known to be a soft rock with high and variable porosity (14-52 %), and consequently, a

wide variation in the petrophysical properties was observed, as referenced in previous studies [8, 28]. Its textural variety was also discussed in previous studies [6, 27].

3. Materials and methods

For studying the stability of the pillar, a couple of processes needed to be done, from fieldwork to modelling, as well as laboratory work. The fieldwork was done in Budafok area (southern Budapest), Hungary, which is known for its cellar systems. The sample site is only a part of a huge cellar system with about 50.000 m^2 area, and around this site, there are more cellar systems like this. One part of the cellar system is presented in Figure 2, with the investigated room and pillar, which is signed with a red circle. The hatched area in Figure 2 is the porous limestone pillars, while the white parts are the cellar branches.

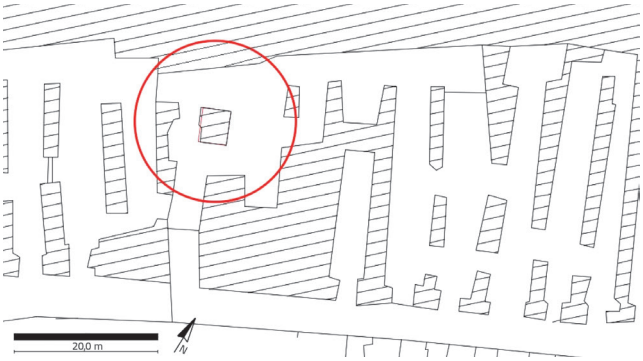

Figure 2. Site plan of the cellar system with the studied pillar; the hatched area refers to the support system

Samples were obtained from the wall of the cellar by drilling (horizontal cores); the drilled cores were 10 cm in diameter, as shown in Figure 3a; later in the laboratory, the 10 cm cores were drilled in a vertical direction to put the specimens into testing as close as possible to the field situation, as shown in Figure 3b. Those cores cut into small specimens around 38.0 mm in diameter. To determine the input data for the modelling, besides the geometry measurements and investigation of the physical properties of the specimens, uniaxial compressive strength (UCS) and triaxial tests (ASTM D 7012-14) has been done. The shear strength test along discontinuities was done according to the instructions of the code ASTM D5607-16. The shear tests have been done under different normal loads.

The geometry of the pillar was obtained manually in the cellar. The dimension of the horizontal cross section is 3.6 m x 4.7 m, and the height of the pillar is 5 m. A picture of the studied pillar is presented in Figure 4.

Figure 4. The studied pillar

The existing joints have been studied to determine the joint modelling parameters that can best represent the joints in the model. The joints in the area have been studied, and the orientation of the major joints was measured using a geological compass and the Rocklogger android application. The measured data was evaluated with Rocscience Dips software. The results of the joint orientations are presented in Figure 5, where the average dip direction is 283 deg and the average dip angle is 77 deg for the main joint set. The joint sets mainly contain very steep joints, but there are some individual joints with lower dip angles as well. In the pillar only one joint from the main joint set can be recognised. Still, in the calculation different joint orientations are also considered for mapping the effect of it on the stability. The 3D model of the studied pillar created in the RS3 software is presented in Figure 6, where the joint has a dip angle of 30 deg.

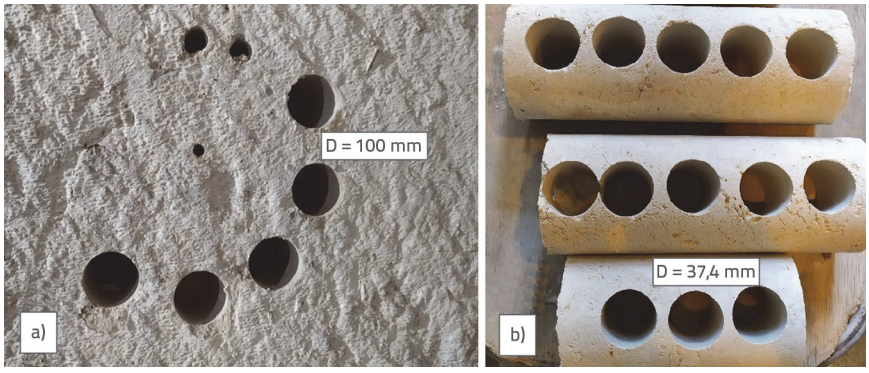

Figure 3. a) The place of obtaining samples in the cellar, b) drilled cores in the lab

Around the cavities the condition of the porous limestone is good and there are some joints that should be considered as well; therefore, for calculating the input parameters of the numerical modelling, the intact rock and joint data were used. For determining intact rock shear strength parameters triaxial tests and direct shear strength tests for joint parameters were done. The results of both tests were analysed using RSData software. The number and results of the basic strength tests (UCS and Brazilian

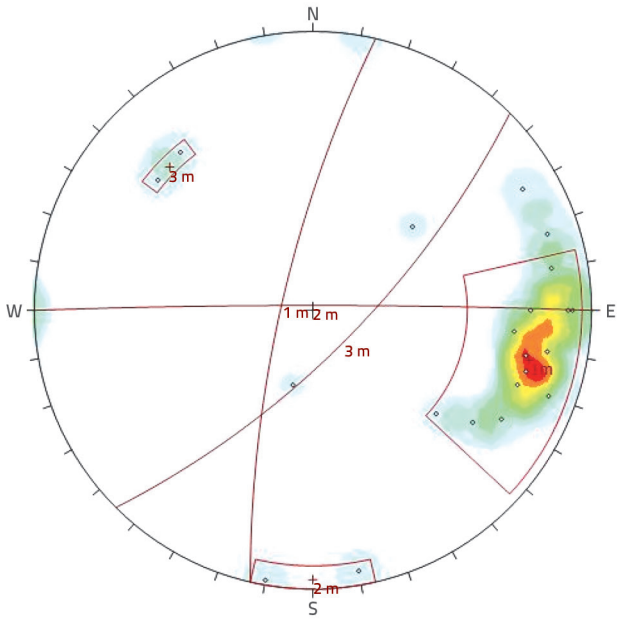

Figure 5. Joints of the studied area with the major joint set

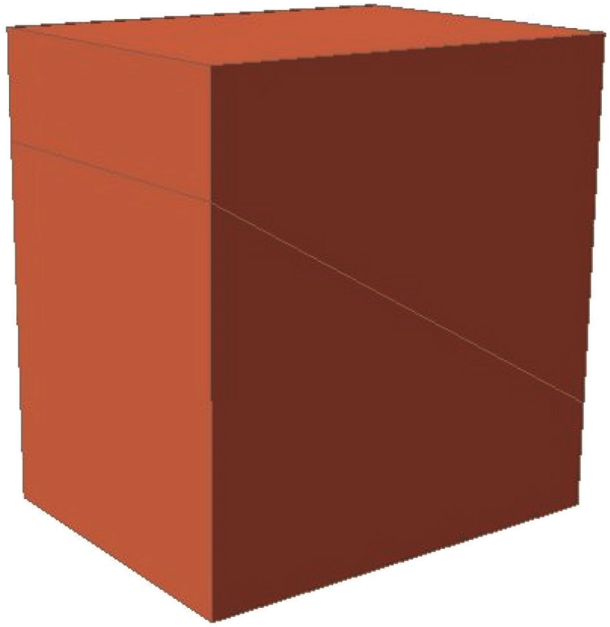

Figure 6. 3D model created by RS3

tensile strength) and density parameters which were tested under laboratory conditions, are visible in Table 1. According to the results the host rock of the cellars is a low-strength soft rock. The International Society for Rock Mechanics (ISRM) raised the definition of soft rock in (1981) based on UCS, a rock with a UCS range of 0.25-25 MPa is classified as extremely weak to weak rock [29].

Table 1. The results of strength tests and density parameter

	UCS [Mpa]	Brazilian [Mpa]	Density [kN/m³]
No. of tests	10	6	37
Min	1.90	0.34	14.0
Average	4.03	0.65	16.6
Max	7.66	0.86	18.5

After determining the failure points in triaxial and UCS tests, all the data were processed in RSData software to obtain the data for modelling. The results were plotted in the minor and major principal stress diagram as presented in Figure 7, the red points refer to measured peak values, while the blue line represents the fitted failure curve (Hoek-Brown).

The Generalized Hoek-Brown failure criterion is used as it is widely accepted to determine the strength parameters of rock masses and has been used in projects worldwide [30, 31]. The mi parameter was calculated from the triaxial data. The input parameters for the rock mass of the porous limestone are listed in Table 2 with variable data such as the width and height ratio of the pillar and the dip angle of the joints. The Young Modulus for intact rock was determined by UCS test with axial displacement measurements. The deformation modulus for the rock mass was calculated by the equation of Hoek and Diederichs.

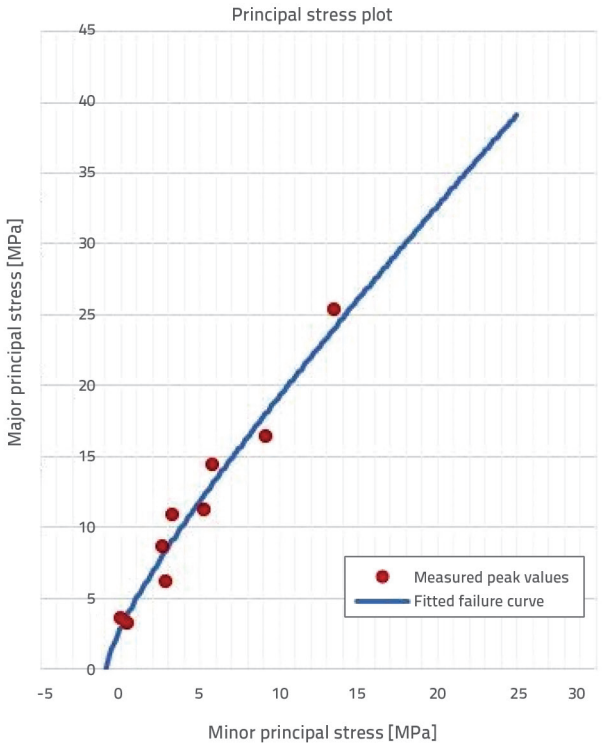

Figure 7. Triaxial laboratory test results plotted on minor and major principal stress diagram

Table 2. Modelling parameters of the intact rock and rock mass, pillar and joint with their range

Parameter	Range
UCS	2.54 [MPa]
GSI	75
mi	3.315
Ei	0.616252 [GPa]
Density	16.6 [kN/m^3]
H (Height of the pillar)	5 m
W/H (width / height)	(0.72, 0.7, 0.6, 0.5, 0.4, 0.3)
Dip angles of joint	(0, 15, 30, 45, 60., 75, 90)

Several direct shear strength tests were done to determine the shear strength along the discontinuities of porous limestone. The used device was a Controls shear box for discontinuities shear strength test with load sensors for measuring normal load and shear load up to 50 kN, the used transducer for measuring shear displacement was able to measure up to 100 mm. The angle of friction and the apparent cohesion were determined, and the results of the tests were plotted on the normal stress–shear stress diagram with the fitting line as shown in Figure 8. In the Figure 8 the red points refer to measured peak values, and the blue line refers to Mohr-Coulomb failure criterion. The angle of friction was 23 deg, and the apparent cohesion was 0.30 MPa. The used peak and residual shear strength values are in Table 3. For the calculation, reduced parameters were also used to model the effect of the water seepage, since the cellars were wet several times because of the failure of water supply pipes. This is the reason for the two different joint shear strength parameters in Table 3, the joints have high persistence as it is in the range of (10-20) m long.

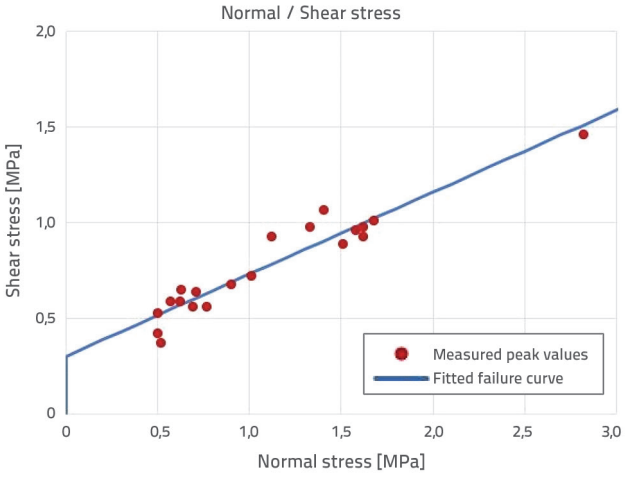

Figure 8. Shear strength tests result along discontinuities of the porous limestone (Normal stress – Shear stress plot)

Table 3. Shear strength parameters of the joints for the model in dry (Joint_1) and wet conditions (Joint_2)

Joints		Peak	Residual
Joint 1	Cohesion [MPa]	0.3	0
	Friction angle [°]	23	33
Joint 2	Kohezija [MPa]	0.15	0
	Cohesion [MPa]	12	15

4. Modelling

The 3D model was built considering the pillar, and the weight of the porous limestone, which loads the pillar considering the dimensions of the room, was calculated separately. Finally, the weight of the porous limestone and the surface load was applied to the pillar as loading. There is a 5 m cover above the roof of the cellar until the surface. This cover layer contains porous limestone with different conditions, and only around 0.5 m thick layer below the surface can be considered as soil cover as in Figure 9.

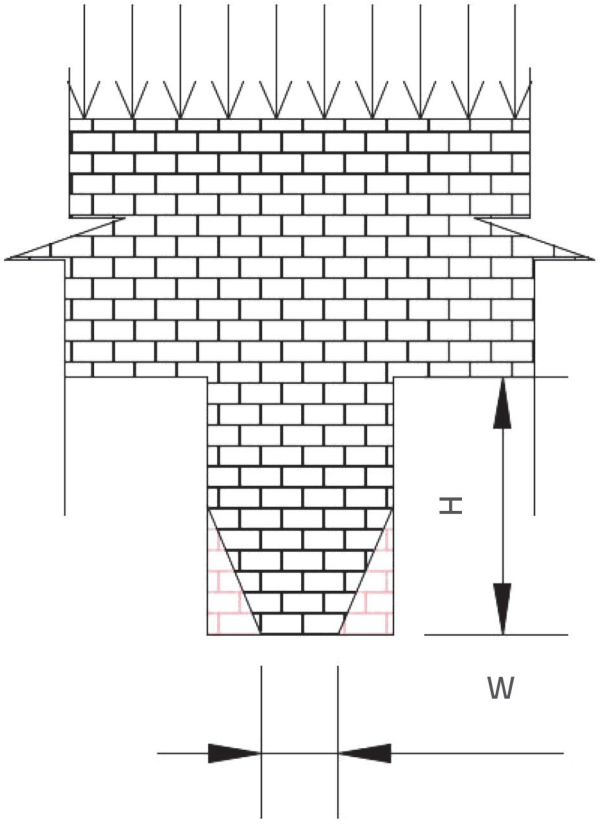

Figure 9. The cross-section of the studied pillar with the rock layer above it

To study the stability and the displacements of the pillar itself without any affection of the layer above it, the 5 m cover layer is considered with 0.123 MPa load, in addition to the building load - the weight of the building which planned to be constructed

- above the cellar is 0.150 MPa. The weight of the porous limestone with the thin soil layer was calculated with an average weight of 16.6 kN/m^3 to determine the load on the pillar.
The modelling studied the effect of two parameters: the values of the dip angle of the joint and the width of the pillar (w) as a W/H ratio (width / height). Each pillar size was modelled with two different geometries; the first is the original geometry,the second is a cut geometry which is similar to the pillars in Figure 1. So, the pillar is studied through the modelling in three stages: first one as original geometry of the pillar with the the joint, second stage after the side cutting, and third stage with loading. The model of the pillar after side cutting and joint is presented in Figure 10. The joint cut the columnar pillar into two parts, as in Figure 10. In this figure, the joint with a dip angle 45 deg is presented; the upper part of the pillar does not reach the ground, so the shear resistance of the discontinuity is the only parameter which holds the upper part of the pillar.Therefore, the importance of discontinuity shear strength appears.

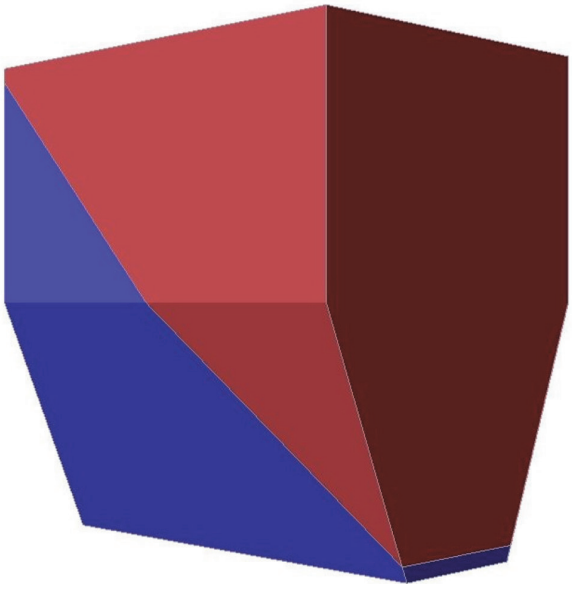

Figure 10. Modell of pillar, which bottom side was cut, with joint (Joint_2, D.A. = 45deg)

Finally, 84 different models were built to determine the results for each case. There are six models to represent the variation of the W/H ratio, and for each W/H ratio, seven models were created to represent the seven different joint dip angles. Each model was run with two different shear strength parameters for the discontinuities. The maximum displacements and the strength reduction factor (SRF) were determined and evaluated for each model. The SRF factor, namely the safety factor, is acceptable when it is bigger than 1.35 [32], since no reduction factor was applied to the shear strength parameters.

5. Result and discussion

All the results are in the following two tables; the results for dry joints (Joint_1) are in Table 4, and wet joints (Joint_2) are presented in Table 5. The first column of the tables shows the joint dip, and the second column shows the W/H ratio. It is the original dimensions; when it is 0.72, the pillar will be thinner in every step. Only slight changes in the displacements exist for the original shape and the cut pillars when only the rock load is applied. However, the effect of the load of the building above the cellar resulted in almost two times higher displacements. The location of maximum displacements is usually in the upper part of the pillar (above the joint) as in Figure 11. the red colour refers to the highest displacements and the blue colour represents the lowest one. The results proved that the cut shape has a higher effect in the case of thinner pillars, so the differences between the displacements in original and cut-shaped pillars are higher. It means that there is a minimum width of the pillar when the cut has no effect, but when the pillar width is smaller than this value, the displacements start to increase when the pillar is cut. This limit is at the W/H = 0.6 ratio under these loading conditions.

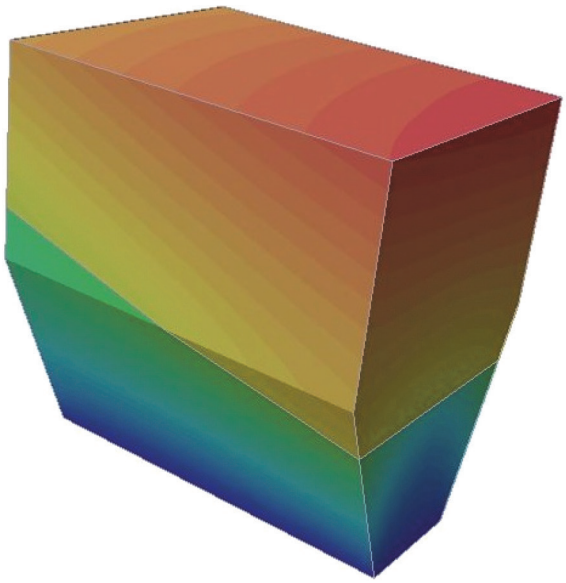

Figure 11. Example for the displacements in the pillar Joint_1 (dry joint parameters), dip angle = 15°, w/h = 0.3

The safety factor was determined only for the cut-shaped pillar with the load of the building., The pillar is safe only below W/H = 0.5 ratio at all joint dips calculating with dry joints (Joint_1 parameters).
When considering the joint with wet condition (Joint_2 parameter), most of the cases resulted with the same displacements and safety factors as in the case of dry joints; because of these cases, the joint has a low effect on the stability because of the advantageous dip. It happens with the dip angle of 0, 15, 75 and 90 deg; in all the other cases, there are some changes. In the case of 30 and 60 deg of dip angle, there is only a slight decrease of safety factors compared to the dry-conditioned joint. The 45 deg joint dip is the most critical; in this case, all the safety factors are below 1.35, so the cellar is unsafe according to this information. When the safety factor is below the SRF = 1.0 limit, the displacements are very high because of the collapse of the cellar.

Table 4. The results of modelling (displacements and SRF) for Joint_1

Dip angle [°]	w/H	Joint 1				Dip angle [°]	w/H	Joint 1			
		Displacement [mm]			SRF			Displacement [mm]			SRF
		Original	Cutting	Building				Original	Cutting	Building	
0	0.72	2.6	2.6	5.2	1.61	60	0.72	2.7	2.7	5.4	1.61
	0.7	2.6	2.6	5.2	1.6		0.7	2.6	2.6	5.4	1.59
	0.6	2.6	2.7	5.3	1.52		0.6	2.6	2.7	5.6	1.51
	0.5	2.6	2.8	5.6	1.4		0.5	2.6	2.8	5.8	1.4
	0.4	2.6	3	6	1.28		0.4	2.6	3	6.1	1.28
	0.3	2.6	3.2	6.7	1.16		0.3	2.6	3.3	6.5	1.16
15	0.72	2.7	2.7	5.4	1.6	75	0.72	2	2	4	1.61
	0.7	2.7	2.8	5.5	1.59		0.7	2	2	4	1.6
	0.6	2.7	2.9	5.7	1.51		0.6	2	2.1	4.2	1.52
	0.5	2.7	3	6	1.38		0.5	2	2.2	4.4	1.41
	0.4	2.7	3.2	6.5	1.28		0.4	2	2.4	4.8	1.3
	0.3	2.7	3.5	7.5	1.16		0.3	2	2.6	5.3	1.17
30	0.72	3	3	5.9	1.6	90	0.72	1.5	1.5	3	1.58
	0.7	3	3.1	5.9	1.59		0.7	1.5	1.5	3	1.57
	0.6	3	3.2	6.3	1.51		0.6	1.5	1.5	3.1	1.49
	0.5	3	3.4	6.7	1.39		0.5	1.5	1.7	3.3	1.38
	0.4	3	3.7	7.3	1.28		0.4	1.5	1.8	3.6	1.28
	0.3	3	4.1	8.6	1.17		0.3	1.5	2	4.1	1.16
45	0.72	3.2	3.2	6.1	1.6						
	0.7	3.2	3.2	6.2	1.59						
	0.6	3.2	3.5	6.6	1.51						
	0.5	3.2	3.8	7.2	1.39						
	0.4	3.2	4.2	8.1	1.28						
	0.3	3.2	4.8	10	1.15						

The calculation results are also represented on a diagram in Figure 12. The two most significant dimensions of the pillar were chosen for the graph. The W/H = 0.6 ratio is the minimum width of the pillar, where the displacements start to increase in the case of the cut-shaped pillar. The other is the W/H = 0.3 ratio, which is the thinnest pillar. The displacements are added to the figure with the joint dip, so the effect of the joint dips is easily visible in the figure. All three cases are shown in the diagram in different colours: the original shape (pink), the cut shape (blue) and finally, the cut shape with building load (green). The black dash-dotted lines represent the scale, the smallest related to 2.5 mm, the middle 5.0 mm, while the biggest shows the 10.0 mm displacement. The figure shows the diagrams for both the dry and wet-conditioned joints. The lowest displacements resulted from the vertical joints and the horizontal ones. The maximum displacements are in the case of 45 deg joints. The wet joint shows the collapse of the pillar when the displacements are increased and the green lines are not connected. In the case of W/H = 0,6 ratio, the displacements of the original and cut-shaped pillars are almost the same, so the pink and blue lines almost overlap. With the other width and height ratio (W/H = 0.3), there are differences even in these two cases as well, so it means that in the case of a thin pillar, the effect of the cut is more significant.

The safety of the pillar is insufficient when the dip angle is 45 deg or when the W/H ratio is smaller than 0.3, so the SRF < 1.35. When SRF < 1,0, the pillar collapses when the dip angle is 45 deg, and the W/H ratio is below 0.6. Fig.13 shows the curve of SRF vs. W/H for both joint conditions when the dip angle is (45deg), all the SRF values of Joint_2 are under 1.35, while for oint_1, two values of W/H (0.4 and 0.3) have lower SRF than 1.35.

The displacements as a function of dip angle when W/H = 0.4 are in Figure 14. the three curves represent the displacements

Table 5. The results of modelling (displacements and SRF) for Joint_2

Dip angle [°]	w/H	Joint 2				Dip angle [°]	w/H	Joint 2			
		Displacement [mm]			SRF			Displacement [mm]			SRF
		Original	Cutting	Building				Original	Cutting	Building	
0	0.72	2.6	2.6	5.2	1.61	60	0.72	2.6	2.6	5.4	1.4
	0.7	2.6	2.6	5.2	1.6		0.7	2.6	2.6	5.4	1.39
	0.6	2.6	2.7	5.3	1.51		0.6	2.6	2.7	5.6	1.36
	0.5	2.6	2.8	5.6	1.4		0.5	2.6	2.8	5.8	1.32
	0.4	2.6	3	6	1.28		0.4	2.6	3	6.1	1.25
	0.3	2.6	3.2	6.7	1.16		0.3	2.6	3.3	6.5	1.15
15	0.72	2.7	2.7	5.4	1.6	75	0.72	2	2	4	1.61
	0.7	2.7	2.8	5.5	1.59		0.7	2	2	4	1.6
	0.6	2.7	2.9	5.7	1.5		0.6	2	2.1	4.2	1.52
	0.5	2.7	3	6	1.38		0.5	2	2.2	4.4	1.41
	0.4	2.7	3.2	6.5	1.28		0.4	2	2.4	4.8	1.3
	0.3	2.7	3.5	7.5	1.16		0.3	2	2.6	5.3	1.17
30	0.72	3	3	5.9	1.44	90	0.72	1.5	1.5	3	1.58
	0.7	3	3.1	5.9	1.43		0.7	1.5	1.5	3	1.57
	0.6	3	3.2	6.3	1.38		0.6	1.5	1.5	3.1	1.49
	0.5	3	3.4	6.7	1.3		0.5	1.5	1.7	3.3	1.38
	0.4	3	3.7	7.3	1.21		0.4	1.5	1.8	3.6	1.28
	0.3	3	4.1	8.6	1.13		0.3	1.5	2	4.1	1.15
45	0.72	3.2	3.2	6.1	1.06						
	0.7	3.2	3.2	6.2	1.05						
	0.6	3.2	3.5	11000	0.99						
	0.5	3.2	3.8	110000	0.92						
	0.4	3.2	4.2	97000	0.85						
	0.3	3.2	4.8	120000	0.77						

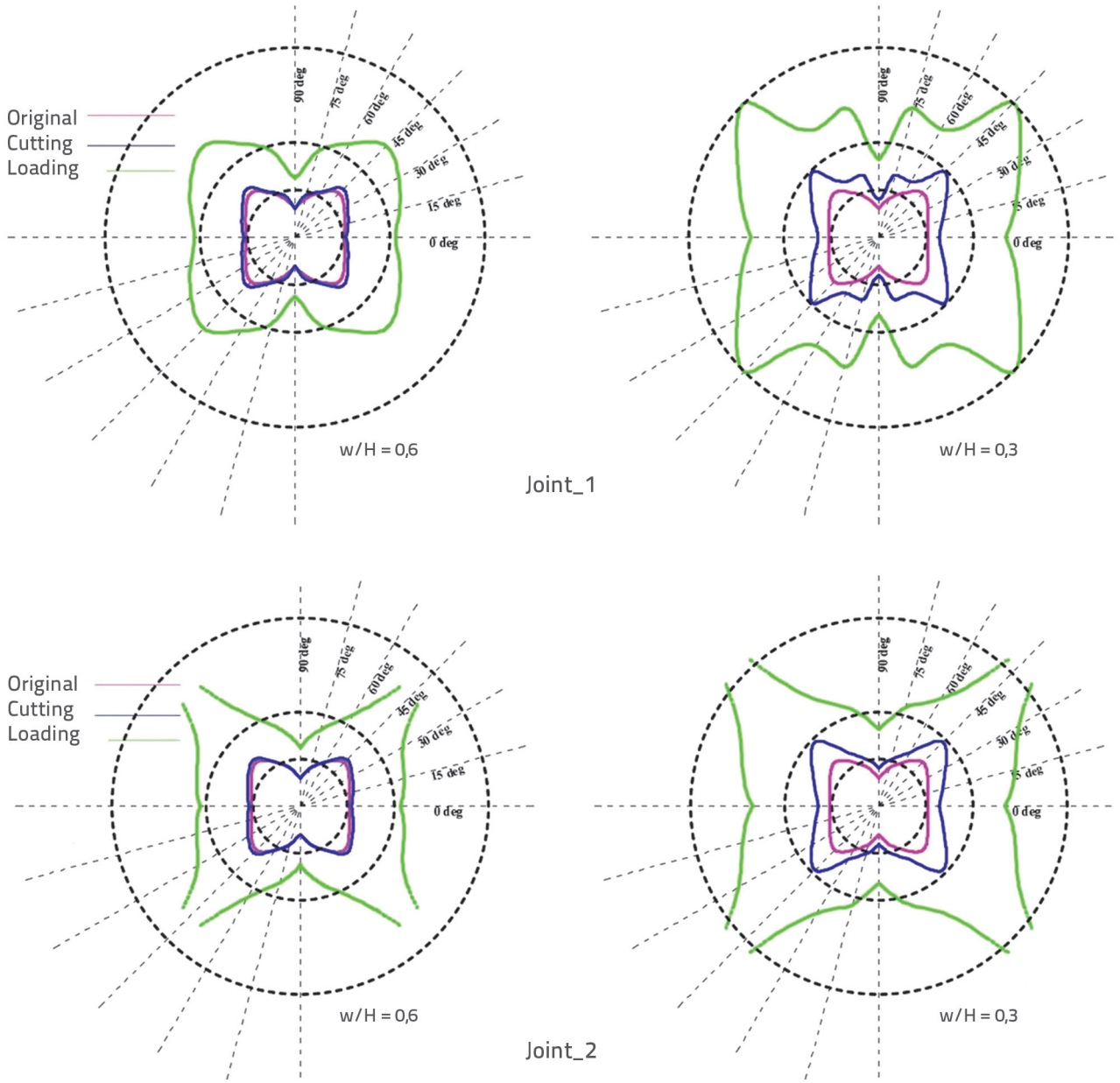

Figure 12. Displacements with the effect of joint dip with different W/H ratios and different joint conditions (the three circles show the scale of displacements in the pillars 2.5 mm, 5.0 mm and 10.0 mm)

of each modelling step. The reduction of the SRF reaches the maximum when we face Joint_2 in dip angle = 45°. this reduction is almost 35 %, as in Figure 15.

Jessu and Spearing [25] studied the strength of a columnar pillar against W/H and the dip angle of the discontinuities. After calibrating the model with the theoretical study of changing W/H, the results showed that the strength of the pillar decreased with decreasing W/H; the same results were found after the current study as in Figure 13, while the dip angle of the joints has a varying effect on the strength of the pillar according to W/H (small W/H leads to less strength), as well as to the results in Fig.14.

Le Quang et. al. [26] studied the effect of pillar width on the stability and displacements of the cellars under a road with a load of traffic, and they found that the decrease in pillar width increases the displacements in the pillar and in the layers above it, which is similar to the results of our study when the displacements increase with decreasing the width for each dip angle, like in Table 4 and Table 5.

One of the most important outcomes of this research is to find the critical dimension of the pillar. If the dimension of the pillar is bigger than this critical one, the cut of the bellow part has no effect on the displacements; if it is smaller, then the displacements increase because of the cut. This result helps to determine if the cut is dangerous to the pillar stability or not. But, this is valid for the conditions studied, which are the same building load and the cellar with the same cover. Under different conditions, the critical dimension of the pillar can be varied.

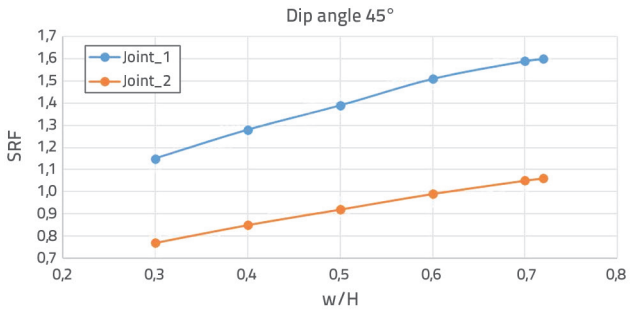

Figure 13. SRF vs. W/H ratio for both joint conditions, dip angle 45°

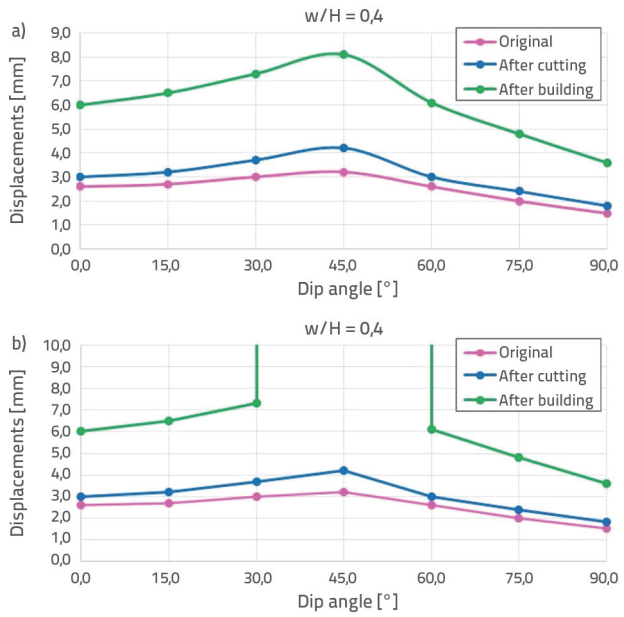

Figure 14. Displacements vs. Dip angle of the joints with both joint conditions in case of W/H = 0.4 ratio: a) Joint_1; b) Joint_2

To evaluate the pillar in Figure 1, the W/H ratio of the pillar is 3,4/5 m = 0.68, the dip angle is around 77°, and the joint properties are similar to Joint_1 (dry joint); according to the results of our study the stability of this pillar is close to the highlighted rows in Table 4.

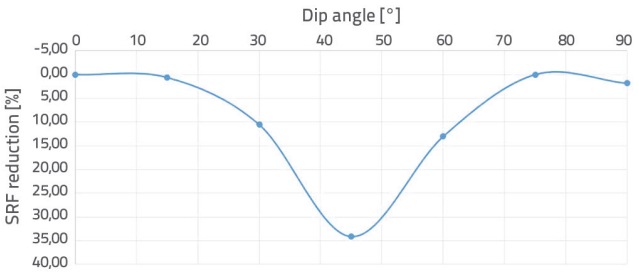

Figure 15. The reduction of SRF for the original width of the pillar and Joint_2

6. Conclusion

Based on the investigations and 3D modelling work, the safe and unsafe conditions of the pillar are presented and discussed, which will help to have a decision in an early stage about the stability of pillars located in the same area. The results showed that for the current strength of the joints, the pillar is safe in the range of W/H, which is (0.72-0.5), with H being the height of the pillar, which is equal to 5 m. But if the W/H ratio is below 0.4, the long-term stability of the pillar cannot be proved because the safety factor SRF < 1.35. The measured joint dip angle in the pillar is around 75°, but the joint dip does not affect the strength in this case because the joint shear strength is high enough.

But, in the case of decreasing joint shear strength, because of the water seepage, the joints' dip angle affects the pillar's safety; when the dip angle is 45 deg, the current condition of the pillar is questionable.

It is important to note that the safety of the pillar is compromised when the width reduction hits the ratio W/H = 0.5, with H = 5 m, under all conditions. Therefore, any reduction in the width of the pillar should be avoided to ensure its safety and stability. Overall, the investigation and 3D modelling work findings can provide useful information to make informed decisions about the pillars in the same area.

Acknowledgment

The research reported in this paper is part of project no. BME-NVA-02, implemented with the support provided by the Ministry of Innovation and Technology of Hungary from the National Research, Development and Innovation Fund, financed under the TKP2021 funding scheme.

REFERENCES

[1] Li, Y., Liu, L., Zhang, J., Liu, C., Zhang, M., Wang, X.: Stability analysis of underground pillar supporting system under different disturbed stresses, Geofluids, (2021) 6, pp. 1–19, doi: 10.1155/2021/6634673.

[2] Mark, C., Agioutantis, Z.: Analysis of coal pillar stability (ACPS): A new generation of pillar design software, Int. J. Min. Sci. Technol., 29 (2019) 1, pp. 87–91, doi: 10.1016/j.ijmst.2018.11.007.

[3] González-Nicieza, C., Álvarez-Fernández, M.I., Menéndez-Díaz, A., Álvarez-Vigil, A.E.: A Comparative analysis of pillar design methods and its application to marble mines, Rock Mech. Rock Eng., 39 (2006) 5, pp. 421–444, doi: 10.1007/s00603-005-0078-z.

[4] Đokić, N., Duranović, M., Lapčević, V., Torbica, S., Petrović, M., Savić, L.: Proposal of 2D finite element model for square pillar stability analysis, Podzemni Rad., 33 (2018), pp. 31–40, doi: 10.5937/PodRad1833031D.

[5] Reed, G., Mctyer, K., Frith, R.: An assessment of coal pillar system stability criteria based on a mechanistic evaluation of the interaction between coal pillars and the overburden, Int. J. Min. Sci. Technol., 27 (2017) 1, pp. 9–15, doi: 10.1016/j.ijmst.2016.09.031.

[6] Pápay, Z., Török, Á.: Effect of thermal and freeze-thaw stress on the mechanical properties of porous limestone, Period. Polytech. Civ. Eng., 62 (2017) 2, pp. 423–428, doi: 10.3311/PPci.11100.

[7] Zenah, J., Görög, P., Török, Á.: Stability of underground excavation in porous limestone: Influence of water content, Acta Montan. Slovaca, 25 (2020) 3, pp. 337–349, doi: 10.46544/AMS.v25i3.7.

[8] Vásárhelyi, B.: Statistical analysis of the influence of water content on the strength of the miocene limestone, Rock Mech. Rock Eng., 38 (2005) 1, pp. 69–76, doi: 10.1007/s00603-004-0034-3.

[9] Hoek, E., Marinos, P., Benissi, M.: Applicability of the geological strength index (GSI) classification for very weak and sheared rock masses: The case of the Athens Schist Formation, Bull. Eng. Geol. Environ., 57 (1998) 2, pp. 151–160, doi: 10.1007/s100640050031.

[10] Somodi, G., Krupa, Á., Kovács, L., Vásárhelyi, B.: Comparison of different calculation methods of Geological Strength Index (GSI) in a specific underground construction site, Eng. Geol., 243 (2018), pp. 50–58, doi: 10.1016/j.enggeo.2018.06.010.

[11] Mathey, M.: Modelling coal pillar stability from mine survey plans in a geographic information system, J. South. Afr. Inst. Min. Metall., 118 (2018) 2, pp. 157–164, doi: 10.17159/2411-9717/2018/v118n2a9.

[12] Lin, H., Yang, R., Li, Y., Fang, S.: Stability of coal pillar and roof movement characteristics in roadway backfill mining, Adv. Civ. Eng., (2021) 3, pp. 1–13, doi: 10.1155/2021/5588923.

[13] Ziwei, D., Jindui, J., Amirohossein, B., Ji, L., Yue, S.: Mechanism and control of spalling for friable sandstone pillars in a room and pillar mine, J. Eng. Sci. Technol. Rev., 11 (2018) 6, pp. 197–205, doi: 10.25103/jestr.116.25.

[14] Arthur, F.A., Ge, M.: Numerical approach to predict the strength of St. Peter sandstone pillars acted upon by vertical loads– A case study at Clayton, IA, USA., IOSR J. Eng., 5 (2015) 1, pp. 36–41

[15] Arzúa, J., Alejano, L., Clérigo, I., Pons, B., Méndez, F., Prada, F.: Stability analysis of a room & pillar hematite mine and techniques to manage local instability problems, Rock Engineering and Rock Mechanics: Structures in and on Rock Masses, CRC Press, 2014., pp. 1147–1152, doi: 10.1201/b16955-198.

[16] Sherizadeh, T., Kulatilake, P.H.S.W.: Assessment of roof stability in a room and pillar coal mine in the U.S. using three-dimensional distinct element method, Tunn. Undergr. Space Technol., 59 (2016) 10, pp. 24, doi: 10.1016/j.tust.2016.06.005.

[17] Tzalamarias, M., Tzalamarias, I., Benardos, A., Marinos, V.: Room and pillar design and construction for underground coal mining in Greece, Geotech. Geol. Eng., 37 (2019) 3, pp. 1729–1742, doi: 10.1007/s10706-018-0717-2.

[18] Kim, J.G., Abdellah, W.R., Yang, H.S.: Parametric stability analysis of pillar performance at Nohyun limestone mine, South Korea—A case study, Arab. J. Geosci., 12 (2019) 12, p. 390, doi: 10.1007/s12517-019-4550-6.

[19] Castro-Caicedo, A.J., Alejano, L.R., Monsalve Oliveros, J.E., Bernal Montiel, A.: Geotechnical design of pillars in underground mines of gold veins in cases of Colombia, DYNA, 86 (2019) 4, pp. 337–346, doi: 10.15446/dyna.v86n209.74041.

[20] Chen, T., Mitri, H.S.: Strategies for surface crown pillar design using numerical modelling – A case study, Int. J. Rock Mech. Min. Sci., 138 (2021) 2, pp. 104599, doi: 10.1016/j.ijrmms.2020.104599.

[21] Song G., Yang, S.: Probability and reliability analysis of pillar stability in South Africa, Int. J. Min. Sci. Technol., 28 (2018) 4, pp. 715–719, doi: 10.1016/j.ijmst.2018.02.004.

[22] Sharma, P., Verma, A.K., Gautam, P.: Stability analysis of underground pillar in the presence of overlying dump: A case study, Arab. J. Geosci., 13 (2020) 5, pp. 217, doi: 10.1007/s12517-020-5133-2.

[23] Esterhuizen, G.S., Tyrna, P.L., Murphy, M.M.: A case study of pillar collapse at a limestone mine in Pennsylvania, Proceedings of The 52nd US Rock Mechanics Geomechanics Symposium, American Rock Mechanics Association, Washington, USA, 2018., p. ARMA-2018-363.

[24] Doležalova, M., Zemanova, V., Danko, J., Kovacs, L.: Convergence measurement and numerical modeling of the rock mass, Građevinar, 52 (2000) 3, pp. 153–142, 2000.

[25] Jessu, K.V., Spearing, A.J.S.: Performance of inclined pillars with a major discontinuity, Int. J. Min. Sci. Technol., 29 (2019) 3, pp. 437–443, doi: 10.1016/j.ijmst.2018.09.006.

[26] Le Quang, P., Zubov, V., Duc, T.P.: Design a reasonable width of coal pillar using a numerical model: A case study of Khe Cham Basin, Vietnam, E3S Web Conf., 174 (2020), p. 01043, doi: 10.1051/e3sconf/202017401043.

[27] Török, Á., Siegesmund, S., Müller, C., Hüpers, A., Hoppert, M., Weiss, T.: Differences in texture, physical properties and microbiology of weathering crust and host rock: A case study of the porous limestone of Budapest (Hungary), Geol. Soc. Lond. Spec. Publ., 271 (2997) 1, pp. 261–276, doi: 10.1144/GSL.SP.2007.271.01.25.

[28] Zenah, J., Török, Á., Rehány, N., Görög, P.: Investigation of the effect of construction activities to underground cavities cut into porous limestone, Proceedings of the ISRM Specialised conference and 8th Conference of Croatian Geotechnical Society - Geotechnical Challenges in Karst, Omiš, Croatia, 2019., pp. 453-458

[29] He, M.: Latest progress of soft rock mechanics and engineering in China, J. Rock Mech. Geotech. Eng., 6 (2014) 3, pp. 165–179, doi: 10.1016/j.jrmge.2014.04.005.

[30] Hoek, E., Carranza-Torres, C., Corkum, B.: Hoek-Brown failure criterion - 2002 Edition, Proceedings of the NARMS-TAC Conference, Toronto, 2002, pp. 267-273

[31] Vásárhelyi, B., Davarpanah, M.: Influence of Water Content on the Mechanical Parameters of the Intact Rock and Rock Mass, Period. Polytech. Civ. Eng., (2018) 10, doi: 10.3311/PPci.12173.

[32] EN 1997-1: Eurocode 7: Geotechnical design - Part 1: General rules, 2004.